

1 **POST FLOODING DAMAGE ASSESSMENT OF EARTH DAMS**  
2 **AND HISTORICAL RESERVOIRS USING NON-INVASIVE**  
3 **GEOPHYSICAL TECHNIQUES.**

4 

---

Philippe Sentenac<sup>a</sup>, Vojtech Benes<sup>b</sup>, Vladimir Budinski<sup>b</sup>, Helen Keenan<sup>a</sup>, Ron Baron<sup>a</sup>

5 **AFFILIATIONS:**

6 <sup>a</sup> Department of Civil and Environmental Engineering, University of Strathclyde,  
7 Glasgow, G11XJ, UK

8 <sup>b</sup> G IMPULS Praha s.r.o., C/ 28073, Nerudova 232, 252 61 Jeneč, Czech Republic.

9 **KEY WORDS:** Electrical Resistivity Tomography, Electromagnetic profile, Self  
10 Potential, Gravimetry, Reservoirs, Embankments.

11

12 **CORRESPONDING AUTHOR:**

13 Philippe Sentenac

14 University of Strathclyde

15 Department of Civil and Environmental Engineering

16 John Anderson Building

17 75 Montrose Street

18 G1 1XJ Glasgow, UK

19 email: [philippe.sentenac@strath.ac.uk](mailto:philippe.sentenac@strath.ac.uk)

20 Phone: +441415484751

1  
2  
3  
4  
5  
6  
7  
8  
9  
10

## Highlights

- Combined Electrical Resistivity Tomography (ERT) with electromagnetic self-potential and microgravimetry to assess reservoir dam integrity
- Validation of Geophysical techniques for detecting damages and seepage in reservoir embankments
- Time lapse Resistivity subtraction changes in the embankment soil matrix between 2010 and 2013
- Discussion on the effect of pre and post flood conditions on soil resistivity

1 **Abstract**

2

3 This paper describes the use of four geophysical techniques to map the structural  
4 integrity of historical earth reservoir embankments which are susceptible to natural  
5 decay with time.

6 The four techniques that were used to assess the post flood damage were 1. A fast  
7 scanning technique using a dipole electromagnetic profile apparatus (GEM2), 2.  
8 Electrical Resistivity Tomography (ERT) in order to obtain a high resolution image of  
9 the shape of the damaged/seepage zone, 3. Self-Potential surveys were carried out  
10 to relate the detected seepage evolution and change of the water displacement  
11 inside the embankment, 4. The washed zone in the areas with piping was  
12 characterised with microgravimetry.

13 The four geophysical techniques used were evaluated against the case studies of  
14 two reservoirs in South Bohemia, Czech Republic. A risk approach based on the  
15 Geophysical results was undertaken for the reservoir embankments. The four  
16 techniques together enabled a comprehensive non-invasive assessment whereby  
17 remedial action could be recommended where required. Conclusions were also  
18 drawn on the efficiency of the techniques to be applied for embankments with wood  
19 structures.

20

21 **Keywords: Slingram; Electrical Resistivity Tomography; Geophysics;**  
22 **Microgravimetry; Seepage; Piping; Earth Dam; Reservoirs**

23

24

25

26

27

28

1

## 2 **1. Introduction**

3

4 Currently only visual inspections are routinely performed to appraise earth flood  
5 embankments condition. Defects however can be masked by the presence of  
6 vegetation and seasonal variations, moisture can reduce fissures or erosion that  
7 were apparent. Previous studies into embankments condition have required the use  
8 of trenching in order to compare surface anomalies with those in the subsurface.  
9 Cooling and Marsland (1954) dug trenches into various embankments following the  
10 1953 flooding in order to examine the effect of fissuring on the soil in breached flood  
11 embankments. Dyer et al (2009) conducted trenching to a depth of 1.5 m in order to  
12 observe the extent of desiccation fissuring.

13 Trenching is a work intensive, time consuming process and destructive to the  
14 embankment structure, there is also a high risk that the trench does not reveal the full  
15 extent of the damage or misses it completely. Geophysical techniques such as  
16 Electrical Resistivity Tomography (ERT) and Electromagnetic scanning have been  
17 suggested as non-invasive methods for examining internal embankment conditions  
18 (Jones 2014, Castellanza 2014, Sentenac 2013, Zielinski 2010). These are among  
19 other Geophysical techniques used to scan embankments. Hadley (1983) used  
20 common offset seismic refraction technique to scan a dam axis and toe. The  
21 anomalous areas were then targeted for drilling. The technique was successfully  
22 applied to about 15 dams in the USA.

23 Modern geophysical surveys often require the use of two or more complimentary  
24 techniques in order to verify the locations of anomalies (Nguyen 2005, McDowell  
25 2002, Reynolds 1997). Sjö Dahl et al. (2006) investigated an embankment in southern  
26 Sweden by taking temperature, ERT, induced polarization (IP) and self-potential (SP)  
27 measurements together with standard visual inspections and piezometer readings.

1 They found that ERT was a good non-destructive technique, which gave the  
2 possibility of detecting internal erosion processes and anomalous seepage at an  
3 early stage before the stability of the dam was compromised.

4 Chao et al. (2006) combined seismic and electric resistivity to locate potential  
5 seepage locations in an embankment along the Yangtze River, in China. They used  
6 S-wave velocity for their seismic profiles to identify anomalies and used the resistivity  
7 profiles to study the moisture content inside the selected embankment. An anomaly  
8 detected in a section of the embankment was verified as a previous location of piping  
9 during flooding in 1998.

10 More recently Cho and Yeom (2007) used ERT to find out anomalous seepage  
11 pathways in an embankment dam in Korea. Two seepage pathways with low  
12 resistivity zones were identified using a dipole-dipole resistivity section obtained from  
13 a line survey along the crest of the dam. One pathway was confirmed by visual  
14 inspection of the dam, and afterward, by trenching.

15 Benes et al. (2011) used the repeated geoelectrical measurement (SLINGRAM, ERT,  
16 SP) during the dry season and flood event for more precise interpretation of  
17 seepages through embankment and dams.

18 Di Prinzio et al (2010) preferred the use of Ground Penetrating Radar (GPR) for the  
19 monitoring of river embankments. Since air-filled voids provided an excellent  
20 dielectric constant contrast, GPR revealed to be suitable for identifying animal  
21 burrows in earthen embankments and levees. The GPR technique is an extensive  
22 investigation method that enables one to rapidly cover a wide area, locating voids  
23 and it is easy to use with the possibility to inspect the collected data in real-time.

24 Nevertheless GPR analysis needs expertise and modeling skills and the  
25 embankments material is also very important. Clay for instance is more difficult to  
26 characterize. Mydlikovski et al (2007) also used high frequency electromagnetic  
27 methods: GPR or measurements of mutual impedance. The depth of penetration of  
28 electromagnetic waves was small due to the fact that, in this medium electromagnetic

1 waves are strongly attenuated. As the structural weaknesses of levee caused by high  
2 level of ground water are characterized by high level of electrical permittivity and low  
3 resistivity, they also used Electrical resistivity Tomography (ERT) to increase the  
4 accuracy of inhomogeneity detection.

5 It is more and more frequent to see in the literature reviews and evaluations of  
6 Geophysical techniques. For example Niederleithinger et al (2012) evaluated  
7 resistivity, electromagnetic, seismic and GPR techniques at a test site along the  
8 Mulde River in eastern Germany, giving advantages and inconvenient of the  
9 techniques reviewed.

10 Although the four techniques used in this study have been used previously and are  
11 described in the literature, it is unusual for more than two techniques to be combined  
12 therefore this is the first study that brings together these four techniques for a  
13 comprehensive non-invasive post flood damage assessment of historical  
14 embankments. An examination of the literature discussing Geophysical techniques  
15 applied to surveying flood embankments have shown the use of ERT to be common,  
16 due in part to the suitability of the construction materials (normally compacted, fine  
17 grained soils) and its sensitivity to changes in moisture as well as its ability to detect  
18 discontinuities in the material.

19 The potential of two conventional Electrical and Electromagnetic methods with  
20 microgravimetry coarse resolution investigation was assessed against two reservoirs  
21 in South Bohemia (Czeque Republic). The electromagnetic survey (EM) was used to  
22 cross check and validate resistivity values and to evaluate quickly possible areas of  
23 high fluctuations in conductivity that may be an indication of structural defect or  
24 piping. The microgravimetry was used for the detection of material transport in the  
25 zone of piping. The interpretation of geophysical measurement was made more  
26 accurate by comparing measurement carried out at the same locations in 2010  
27 (under normal condition) and in 2013 (after flooding).

1  
2  
3  
4  
5  
6  
7  
8

The embankments surveyed were located in South Bohemia, Czech Republic. These dams are historical and were built during the second half of the 16th century. Table 1 summarizes each Geophysical technique, and how they can help for a non intrusive ground investigation prior to trenching and drilling boreholes in the dams.

Table 1. Geophysical techniques used and applications relevance

	Stratigraphy	Voids/cavities	Ground Water	Seepage	Mine Workings	Contamination/ Utilities	Services/ Utilities	Foundations/ obstruction		
<table border="1"><tr><td>Highly applicable</td></tr><tr><td>Partly applicable</td></tr></table>	Highly applicable	Partly applicable								
Highly applicable										
Partly applicable										
ERT	Highly applicable	Highly applicable	Highly applicable	Highly applicable	Partly applicable	Highly applicable	Not applicable	Partly applicable		
Electromagnetics	Not applicable	Not applicable	Highly applicable	Highly applicable	Highly applicable	Highly applicable	Highly applicable	Highly applicable		
Microgravimetry	Not applicable	Highly applicable	Not applicable	Partly applicable	Highly applicable	Not applicable	Not applicable	Not applicable		
Self Potential	Highly applicable	Not applicable	Not applicable							

9

10

## 11 2. Methodology

12 Four complementary geophysical techniques were used to scan the embankments  
13 following the same methodology and procedure.

### 14 2.1 Electromagnetic Surveying

15 The first technique used was the Electromagnetic Slingram profiling which is based  
16 on the measurement of induction of the primary electromagnetic field of the  
17 transmitting coil in the surrounding investigated medium. The primary field induces a  
18 secondary field whose intensity depends on the conductivity (resistivity) of the  
19 medium surrounding the transmitting coil. The depth to obtain the information on the  
20 conductivity of the medium depends on the frequency of the primary electromagnetic

1 field or on the length of the transmitter coils. High frequencies reach lower depth  
2 penetration than low frequencies. The sensor GEM2 (GEOPHEX USA) operating as  
3 broadband digital multi-frequency electromagnetic device was used at 4 frequencies.  
4 These frequencies were selected as the most appropriate, based on the analysis of  
5 electromagnetic noise at the site. The respective frequencies were 6525 Hz, 13025  
6 Hz, 27025 Hz and 47025 Hz. These frequencies represented approximate depth  
7 penetrations of 6 m, 4 m, 2 m and 1 m. The measurements were conducted with  
8 stacking of 5 (i.e. the average of 5 consecutive measurements was stored in the  
9 memory). They were carried out “continually” at a walking pace. The results density  
10 was approximately 3 to 4 scans per 1 m of profile. The device was connected to GPS  
11 navigation, hence recording the measurement positions automatically. The measured  
12 data were analysed with the programme DIKINS\_analyzer (MEASProg – Czech  
13 Republic).

14 The Electromagnetic method (EM) provides significant advantages for shallow  
15 environmental characterization. Unlike seismic or ground-penetrating radar methods  
16 that involve heavy logistics and labour-intensive field work, GEM-2 requires only a  
17 single operator, is contactless with the ground (thus, is less intrusive), and can  
18 operate at stand-off distance. The relative high-frequency signal can travel only a  
19 short distance and thus, "sees" only shallow structures. Therefore, scanning through  
20 a frequency window is equivalent to depth sounding and is particularly interesting for  
21 flood or reservoir embankments.

22

## 23 **2.2 Resistivity Surveying**

24 Electrical resistivity tomography (ERT) is a well-established geophysical technique  
25 that is commonly applied at the ground surface and has particular promise in  
26 complementing conventional methods of site investigation towards spatially improved

1 characterisation of subsurface water, soil layers and pollutant transports (as reviewed  
2 e.g. in Slater, 2007). Aside from delivering improved spatial information, in-situ ERT  
3 surveys are also rapid and cost-effective compared to traditional methods of access-  
4 hole sampling and analysis.

5 The resistivity arrays technique is routinely used to map ground water and  
6 contaminated flows, it is also regularly used to located buried artefacts or structures.  
7 ERT performs particularly well in soils media consisting of clay or silty soils due to the  
8 excellent contact between electrodes and the soil, and the high concentration of  
9 charged particles that facilitate electrolytic conduction through the soil. Modern  
10 resistivity surveys involve the use of computer controlled multi-electrode arrays in  
11 order to efficiently obtain resistivity measurements over the surveyed section. The  
12 inversion of this data with software like Res2dinv or Res3dinv gives a tomography  
13 contour model of the subsurface in two or three dimensions (Griffiths and Barker,  
14 1993).

15 The principle of the method is based on the measurement of the soil resistivity, using  
16 a large number of electrodes placed along the profile or in the area. The electrodes  
17 are interconnected by a special cable that enables to connect the electrodes as  
18 current ones and potential ones step by step. This allows performing the  
19 measurement for a large number of variants of a 4-electrodes array with differing  
20 geometry and penetration depth. The measurement proceeds automatically,  
21 everything is PC-controlled. For the resistivity tomography measurements, the device  
22 ARES (GF Instruments, Czech Republic) was used. The distance between the  
23 electrodes was 2.5 m on longitudinal profiles of the embankments and 1 m on the  
24 perpendicular profiles. 2D resistivity sections were compiled using the programme  
25 Res2Dinv (GEOTOMO Software - Malaysia). A Schlumberger electrode arrays  
26 configuration was chosen for the ERT measurements. The results were collected  
27 using the 3rd iteration of least squares method.

### 1 **2.3 Self-Potential method**

2 The SP method measures the natural electrical potential of soils and rocks. In dam  
3 surveying, the filtration potential produced by water through a porous medium can  
4 often be detected. The principle of this phenomenon consists in unequal mobility of  
5 anions and cations transferred by the liquid medium through the porous material.  
6 This inequality generates measurable negative potential at the point of infiltration  
7 and positive potential at the point of outflow. When interpreting SP potentials, it is  
8 necessary to distinguish a natural filter electric field from interfering fields caused by  
9 the natural electrochemical process or artificial fields (for example near railways,  
10 cables and tubes). The outcomes of the measurement using the SP method are  
11 profile curves – graphs of electric potentials. Based on their analysis, the locations of  
12 potential seepage paths through the levee can be identified. To assess the presence  
13 of seepage, it is convenient to take measurements on the land side during dry  
14 season (decreased water level in the reservoir) and during the flood (maximal water  
15 level in the reservoir). The method is suitable also for repeated – monitoring  
16 measurements aiming to monitor long-term changes in the seepage regime of the  
17 levee and its underlying layers. The measurements were performed with the device  
18 GEOTOR I (Czech Republic), using the non-polarized electrodes with spacing of 2,5  
19 or 5 m.

### 20 **2.4 Microgravimetry**

21 Gravimetric method is sensitive to the changes of bulk densities of the medium at the  
22 point of measurement. This allows assessing places in the dams disturbed by water  
23 seepage or piping with transport of fine soil material. Cavities are most often caused  
24 by sediments washing out along zone of piping or seepage. On the ground surface  
25 there is a risk of occurrence of progressive deformations or sudden collapses. For

1 the measurement, a gravimeter SCINTREX CG5 was used. The step of  
2 measurement was 2 or 4 m.

3 All the gravimetric data were corrected. They were processed to the values of relative  
4 Bouguer anomaly without topographic correction. Therefore, the dam and the profile  
5 position were symmetrical, there were no hills and we were only interested in shallow  
6 local anomalies.

7 A 2,5D density modelling software called MAG with Talwani formula was used. The  
8 software was evaluated by Geofyzika Brno s.p. Differential densities were used,  
9 meaning that the normal mass had density "0" and local gravity anomalies presented  
10 some +/- differential densities.

11 The regional trend of Bouguer anomaly, which corresponds to deeper geological  
12 structures and effect of relief, was calculated on the basis of polynomial regression of  
13 the measured profile data. The difference between the measured data and their  
14 regional trend corresponded to the residual Bouguer anomaly. This anomaly  
15 represented the gravitational effect of shallow deposited dense inhomogeneities. In  
16 our case, it described best the position of the washed zone in the dams. The  
17 residual Bouguer anomaly was used for the modelisation of the density model.

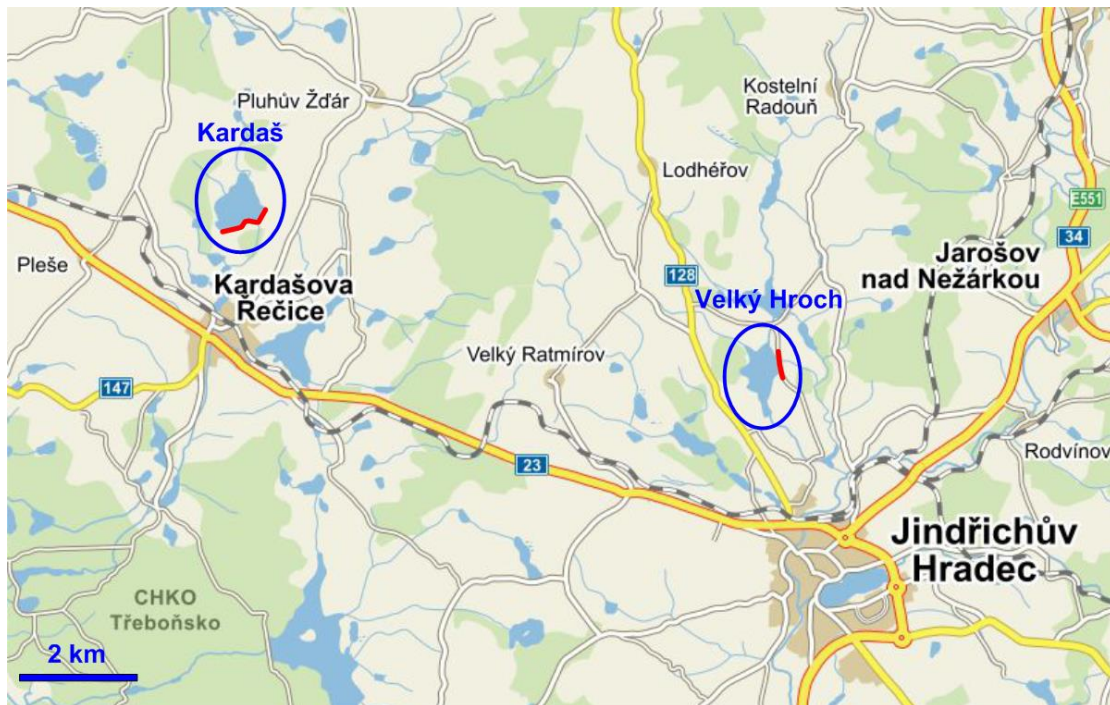
18

19

### 1 3. Surveys Results

2 The geophysical survey of the Velky Hroch reservoir in South Bohemia (Czech  
3 Republic) was made in 2 stages: In October 2010 it was part of the of the project no.  
4 60023529 – Norway grants, and in June 2013 it was part of the current project no.  
5 324426 – MAGIC FP7 – PEOPLE. The aim of the first stage was the characterization  
6 of material homogeneities and the detection of possible weak zones of the  
7 embankment.

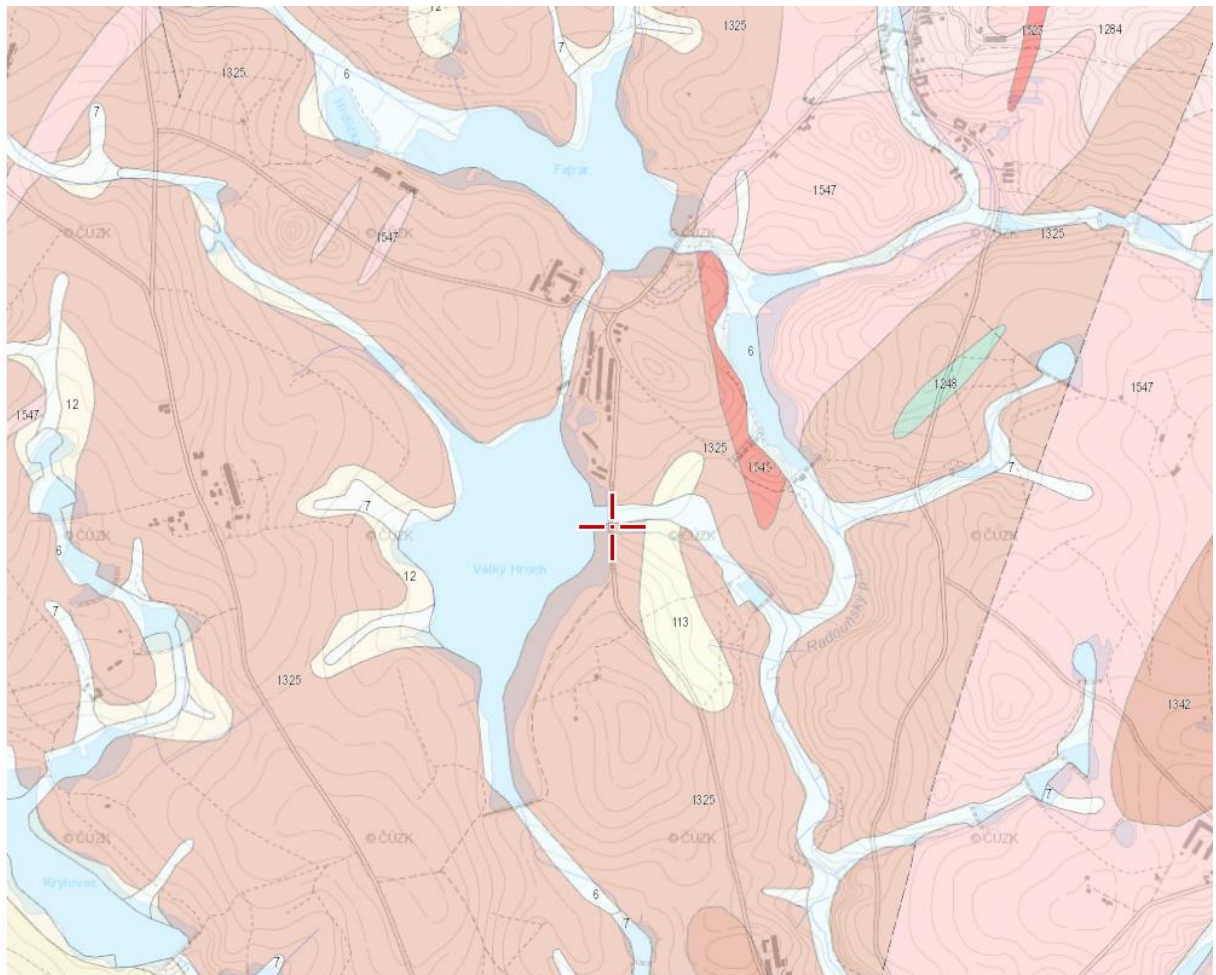
8 A site map indicating the location of all geophysical surveys is presented in Figure 1.



9  
10 Figure 1. South Bohemian ponds and location of all geophysical surveys as red  
11 lines.

12  
13 The Velky Hroch dam was built from material with resistivity ranging from 200 to 300  
14 ohm/m (as seen on resistivity curves of Slingram on Figure 3). It is typical for sandy  
15 clay with higher permeability. The dam dimensions are: lenght app 300 m, max.  
16 elevation app. 7,5 m, slope 1:1,5 to 1:2. The local materials used for the construction  
17 at that time were mainly sand and sandy clay. Oak trees were used to improve the

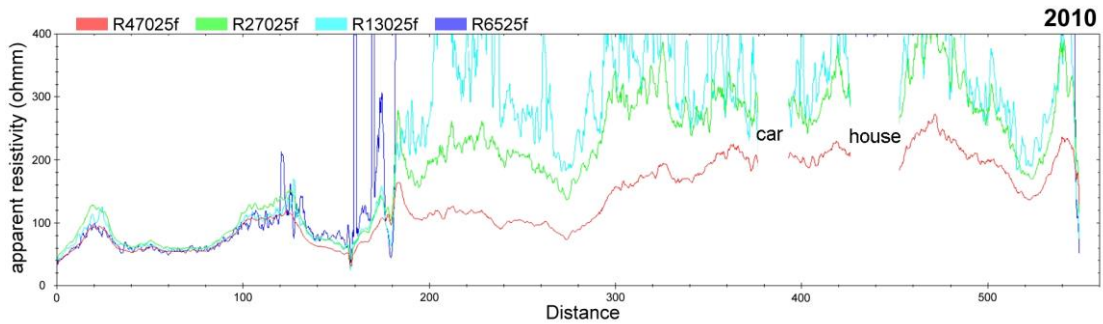
1 stability of the land side slopes. The original outlet was also made from oak wood.  
2 Total replacement was cost prohibitive therefore identification of damage and repair  
3 was the current choice. The Meadow sediment is mainly silty sand and gravel,  
4 clayish sand and gravel with a thickness of approximately 1-3 m. The Bedrock is  
5 made of paragneiss or migmatite. A Geological map is presented on Figure2.



6  
7 Figure 2. Geological map of the Vely Hroch pond. (6: loam, sand, gravel, 12: =  
8 clayish sand, gravel, 1325: paragneiss, migmatite, 113: sandstone, claystone

9  
10 Electromagnetic survey:  
11 Some local decrease of resistivity on the profile near the dam toe was interpreted as  
12 local seepages.

13



1  
2 Figure 3. Graphs of apparent resistivity by Slingram method (GEM-2 sensor).

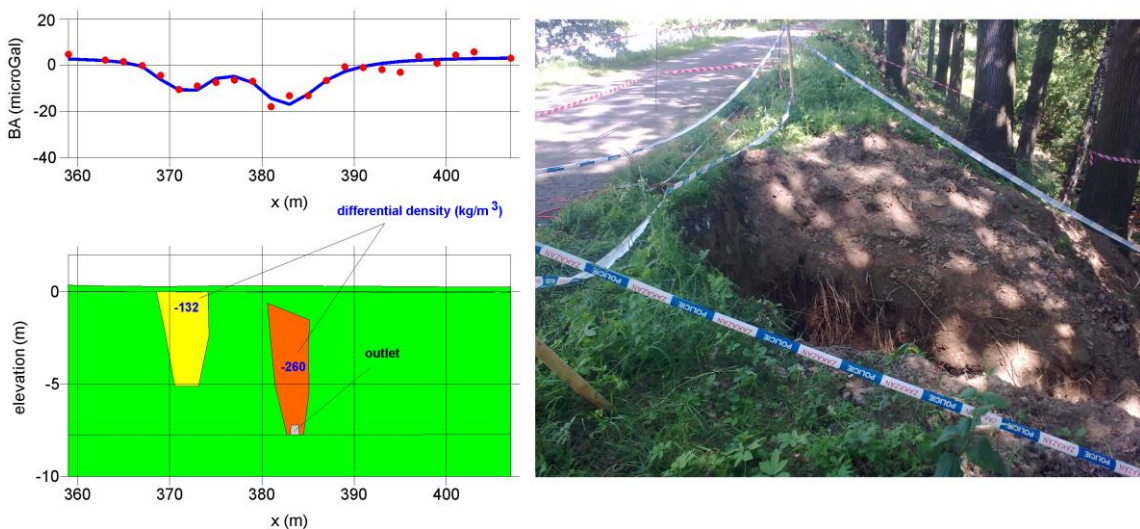
3 Longitudinal Profile in the dam axis, repeated measurement for 2010

4

5 The most concerning anomaly was detected by microgravimetry above the outlet  
6 wood pipe (see Figure 4). The local minimum of residual Bouguer anomaly was  
7 interpreted like a disturbed zone characterised by the washing effect of the water and  
8 the assessment of cavities near the outlet pipe due to piping process.

9

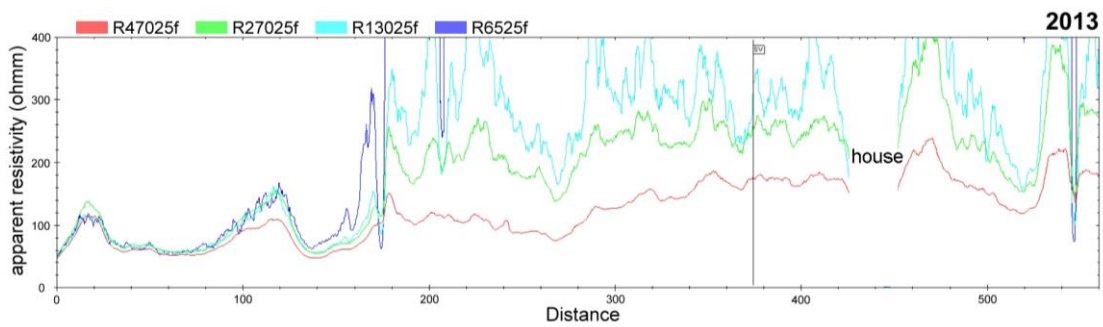
10 The embankment section was therefore categorized with a high risk of breach. This  
11 interpretation was verified during the flood in June 2013 when the collapse of a cavity  
12 occurred on the land side slope of the dam (see corresponding picture in Figure 4).



13

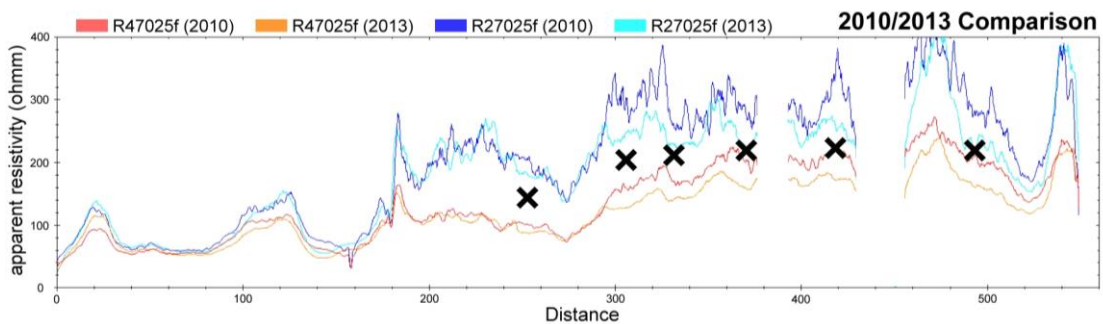
14 Figure 4. Density model by microgravimetric measurement. Profile above the outlet,  
15 detection of piping with cavity in 2010.

1 The second stage of the geophysical survey was arranged after flooding in June  
 2 2013 to see the changes of water saturation in the dam body. The repeated Slingram  
 3 measurement is presented in Figure 5 for 2013. There is a good agreement between  
 4 the initial and repeated measurements. A decrease in resistivity was observed on the  
 5 deviations chart resistivity curves mainly in the central part of the dam near the outlet  
 6 (symbol SV in the middle graph).



7

8 Figure 5. Graphs of apparent resistivity by Slingram method (GEM-2 sensor).  
 9 Longitudinal Profile in the dam axis, repeated measurement for 2013



✘ significant decrease of resistivity after flood (measurement 2013), local seepage

10

11 Figure 6. Comparison of apparent resistivity between 2010 and 2013 by Slingram  
 12 method (GEM-2 sensor). Longitudinal Profile in the dam axis

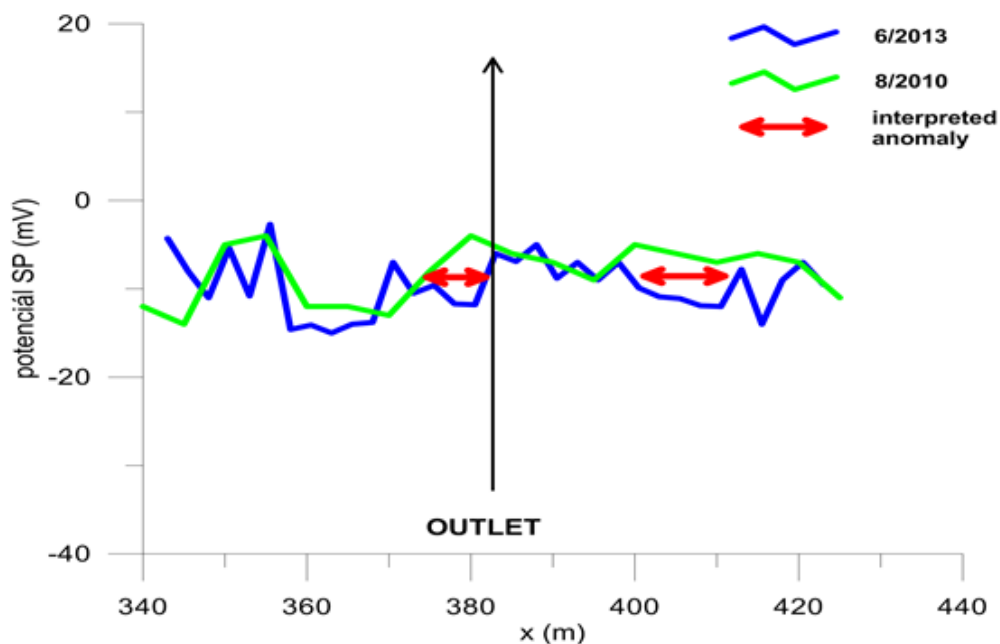
13 The significant anomalies detected on Figure 6 are represented by small crosses and  
 14 they are interpreted as a manifestation of preferential seepage that occurred during  
 15 floods in 2013. The decrease in resistivity here reached 20% of the baseline values.  
 16 In other parts of the dam, residual deviations in resistivity generally decreased by

1 10% of measured values. This can be explained by the effect of higher water  
2 saturation after the flood.

3

4 Self Potential (SP) survey:

5 The seepage detection was checked with SP measurement too. SP curves are  
6 presented on Figure 7 from the profile near the dam toe on the land side. They were  
7 interpreted as two zones of local decrease of SP potential after the 2013 flood. Both  
8 zones are in good correlation with the anomalies detected with the Slingram method.



9

10 Figure 7. Comparative graphs of SP potential between 2010 and 2013. Profiles at the  
11 dam toe, land side (seepage detection).

12

13 Electrical Resistivity Tomography (ERT) survey

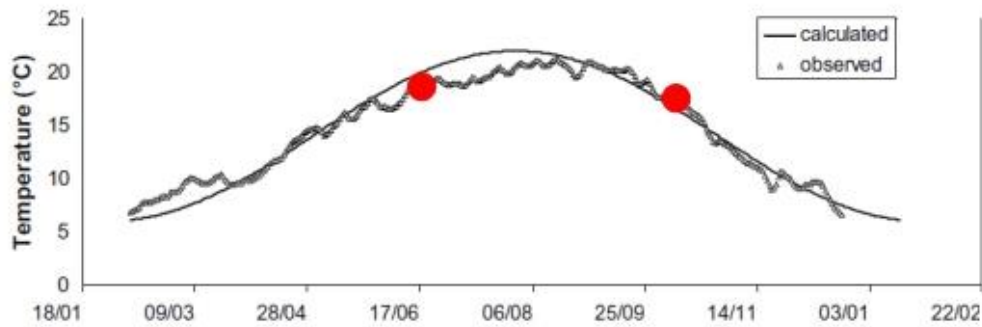
14 Velky Hroch pond:

15 Repeated ERT measurements were carried out for a better description of the  
16 changes in the dam body near the outlet after the 2013 flood and compared with the  
17 2010 surveys.

18 It was assumed that during late spring and early autumn the weather condition was  
19 similar with an air temperature around 20°C. The temperature in the soil at a depth of

1 more than 1 m during the year changed very smoothly with a long delay  
2 (approximately 1 month) similarly to the plot showed in Figure 8 for another survey  
3 exhibiting the same temperature trend line. Therefore it was accepted that the  
4 temperatures changes in the dam body could be neglected and there was no need  
5 for temperature correction in the resistivity data.

6



Example of measured and calculated temperatures at 65 cm depth ( $R^2 = 0.96$ ).

● time of stages geophysical survey (10/2010, 6/2013)

Brunet et al. 2008: Monitoring soil water content and deficit using Electrical Resistivity Tomography (ERT). A case study in the Cevennes area, France. Journal of Hydrology 380 (2010) 146–153.

7  
8

9 Figure 8: Temperature effect on resistivity, related to similar seasonal effect.

10

11 The Schlumberger array configuration was chosen for the ERT survey as it is the  
12 more adequate for the study of geological conditions with mostly horizontal layers.  
13 Earth embankments are generally constructed by horizontal layers and the boundary  
14 of the dam body with bedrock is mostly horizontal too.

15 The position of electrodes was very close during both stages. There were some  
16 geodetic points on the dam to help the layout using the measuring tape. The position  
17 of the profile was 5 m to the side of the outlet and 2 m away from the collapse  
18 boundary at the surface. It has to be noted that it was possible to compare structures  
19 at depth down to 5 m very well if the electrodes position error is less than a 1 m.

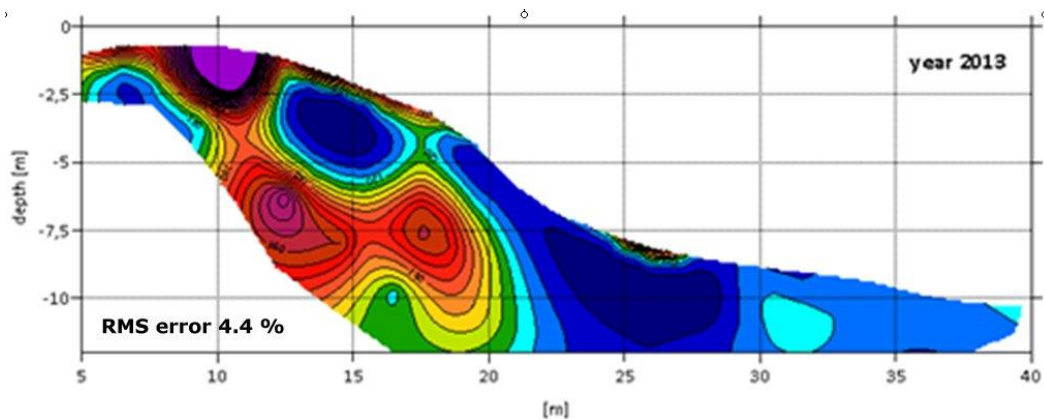
20

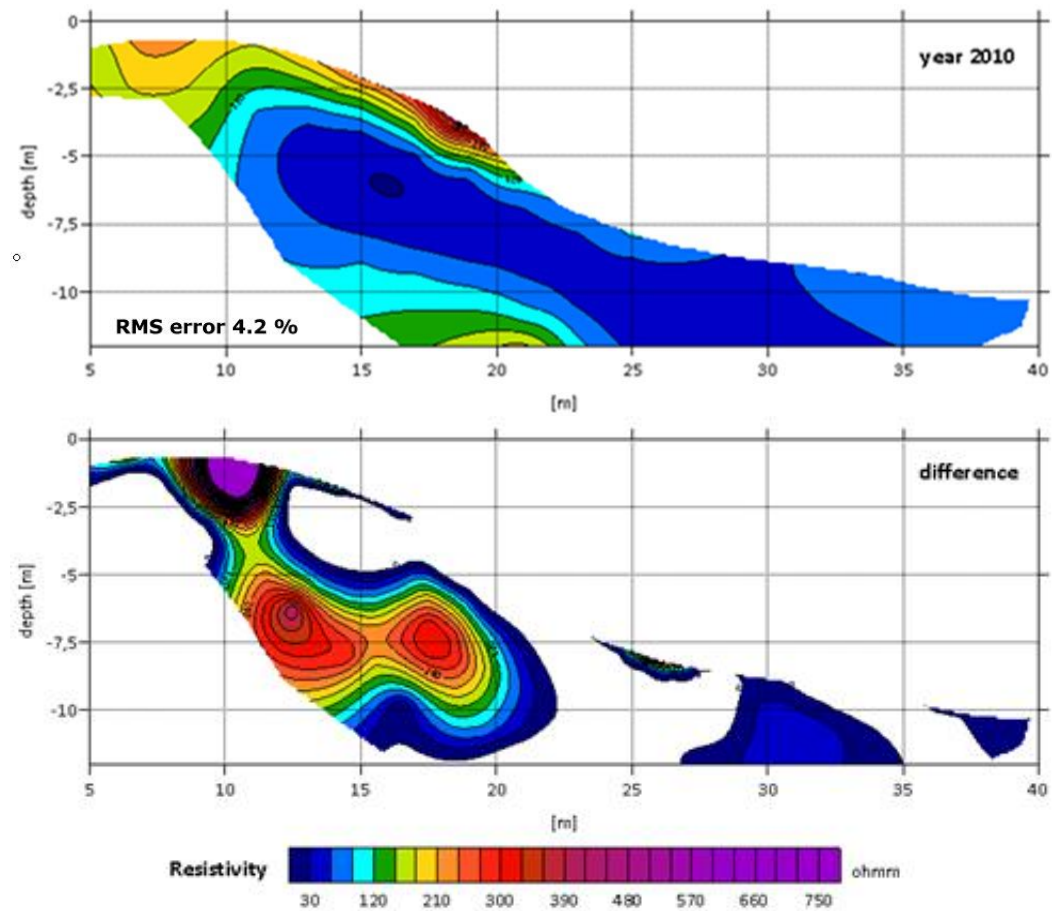
21

1 A L2-norm approach (Standard method) was used. It was assumed that the L1-norm  
2 approach (Robust method) is better for noisy area and for a geological body with  
3 sharp boundary and a much contrasted resistivity.

4 The 3rd iteration used for the inversion offered the best description of normal and  
5 smooth geological conditions based also on the development of the RMS Error.  
6 Usually 5 iterations were carried out. If the difference of RMS Error between 3 and 4  
7 iteration w similar and the value of RMS Error for 3rd iteration is less than 8%, it is  
8 assumed that the model for the 3rd iteration is the closest to real conditions. Using  
9 higher iterations with higher resistivity contrast and shifting the resistivity boundaries  
10 near surface can reduce RMS error but it very often a mathematic effect only.

11 The tomographic subtraction between 2010 and 2013 (Figure 9) revealed some  
12 embankment resistivity changes over time. In general, the ERT results showed also  
13 good agreement between the initial and repeated measurements. The increase in  
14 resistivity located near the surface could be explained by the drying process of the  
15 dam top soil during hot summer time. The collapse of part of the embankment is  
16 shown as a large increase in resistivity (general signature of a cavity). The dam body  
17 around the large increased anomaly presented lower resistivity in year 2013. It could  
18 be explained as the effect of higher water saturation after the flood period. An area of  
19 decreased resistivity in the dam body is clearly visible on the 2010 scan, which is in  
20 good correlation with the curve of the surface water. The “spot” of low resistivity at  
21 the surface near the position 30 show the seepage above the outlet pipe.





1

2

3 Figure 9. Resistivity cross-section by ERT. Perpendicular profile near the outlet,  
 4 scans subtraction for the years 2010 and 2013.

5 The mapping of all interpreted anomalies is shown on Figure 10

6



1

2

3 Figure 10. Mapping of interpreted geophysical anomalies. Repeated measurement  
4 years 2013 – 2010.

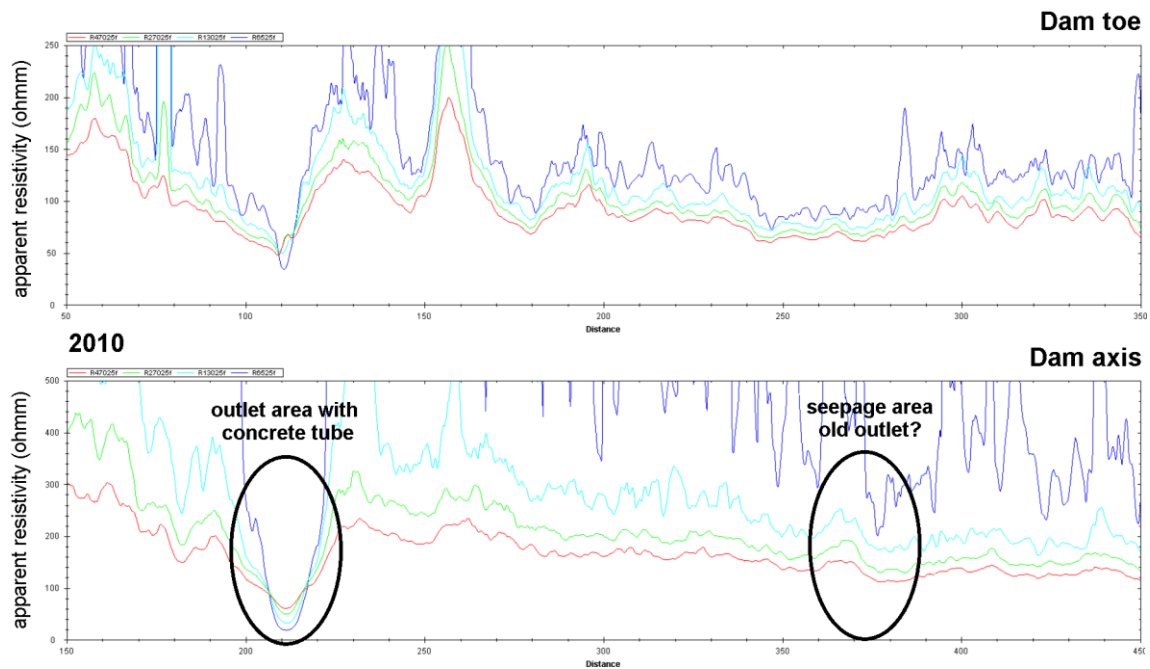
5

6 **Kardas reservoir**

7

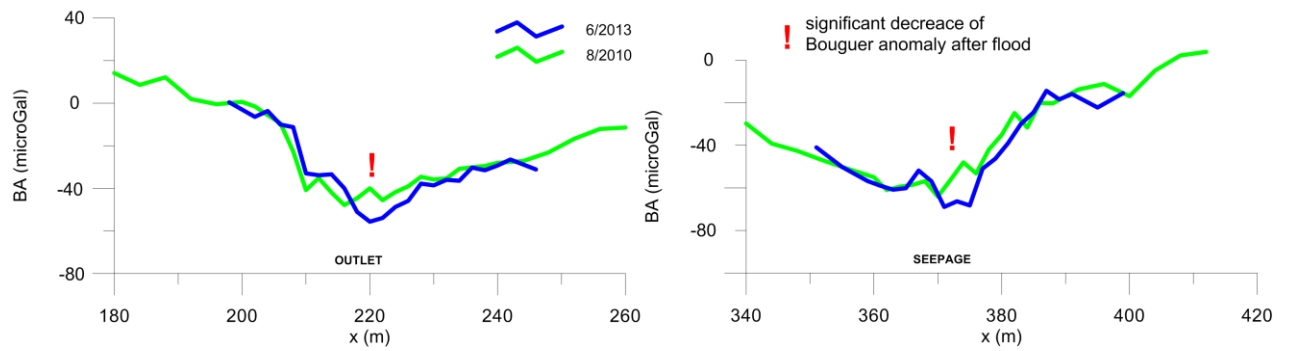
8 The Geophysical survey of Kardas reservoir embankment was carried out following  
9 the same methodology. The dam was built with materials with typical resistivity  
10 ranging from 80 to 400 ohm/m, as shown on the graphs of apparent resistivity  
11 obtained by the Slingram method (The western part of the dam (upper dam) is mainly  
12 made of heterogeneous material (clay sand and gravel). The dam is located in a  
13 shallow valley filled with sediments. The base layer of the dam comes from granites,  
14 gneisses and magmatites. The dam is layered with less permeable local materials

1 (related to the geology characteristics of the dam surroundings). The boundary  
2 between blocks is sub-vertical. The sealed core of the dam is not continuous.  
3 The Slingram fast survey showed on Figure 11 revealed 2 anomalous zones. The  
4 first one was near the main outlet where the dam was dug over and where the outlet  
5 tube was changed. The second anomaly corresponds to a local decrease in  
6 resistivity which was interpreted as the effect of shallow seepages.



7  
8  
9 Figure 11. Graphs of apparent resistivity obtained by Slingram method. Profile along  
10 the dam length.

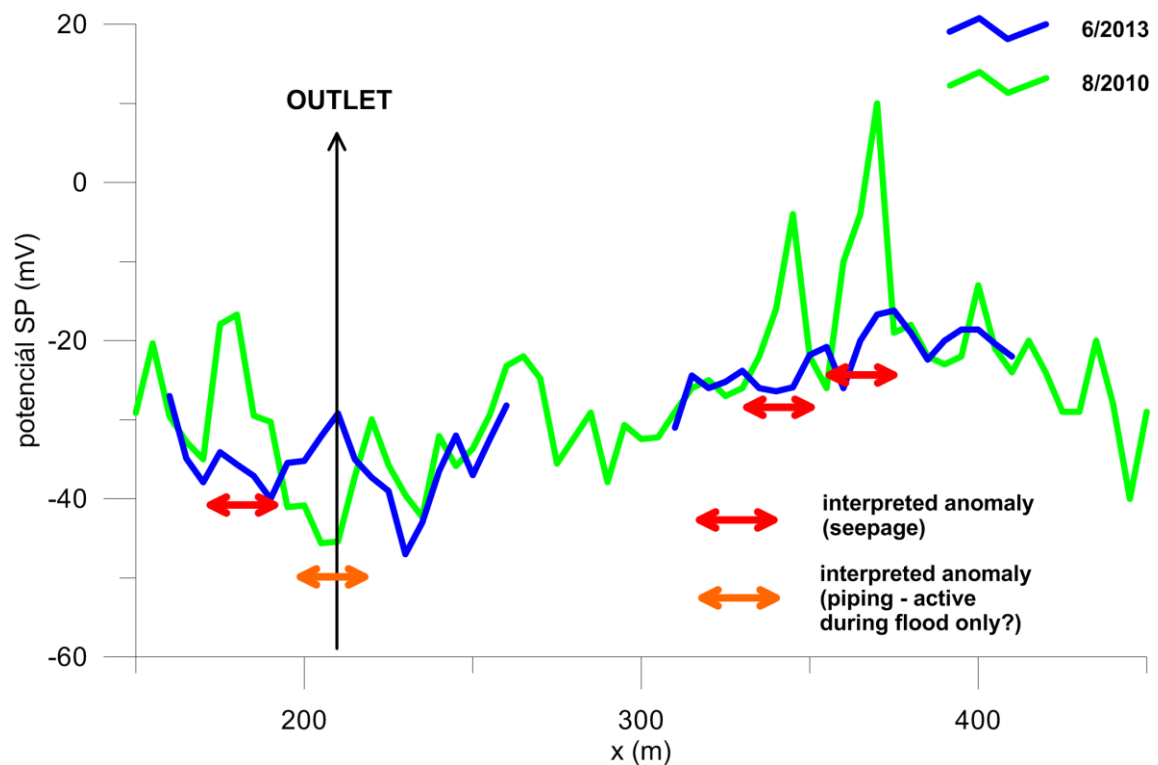
11 For both zones, local microgravimetric measurements (Figure 12) revealed the same  
12 anomaly and can be explained as the effect of density, decreasing. The anomaly was  
13 interpreted the same way as for the Velky hroch dam as a result of material transport  
14 in the piping zone. The anomalies also appear more important after the 2013 flood,  
15 meaning that the piping process was very active during the flood.  
16



1  
2  
3  
4  
5  
6

Figure 12 Repeated microgravimetric measurement. Graphs of Bouguer anomaly. Profiles along the dam axis.

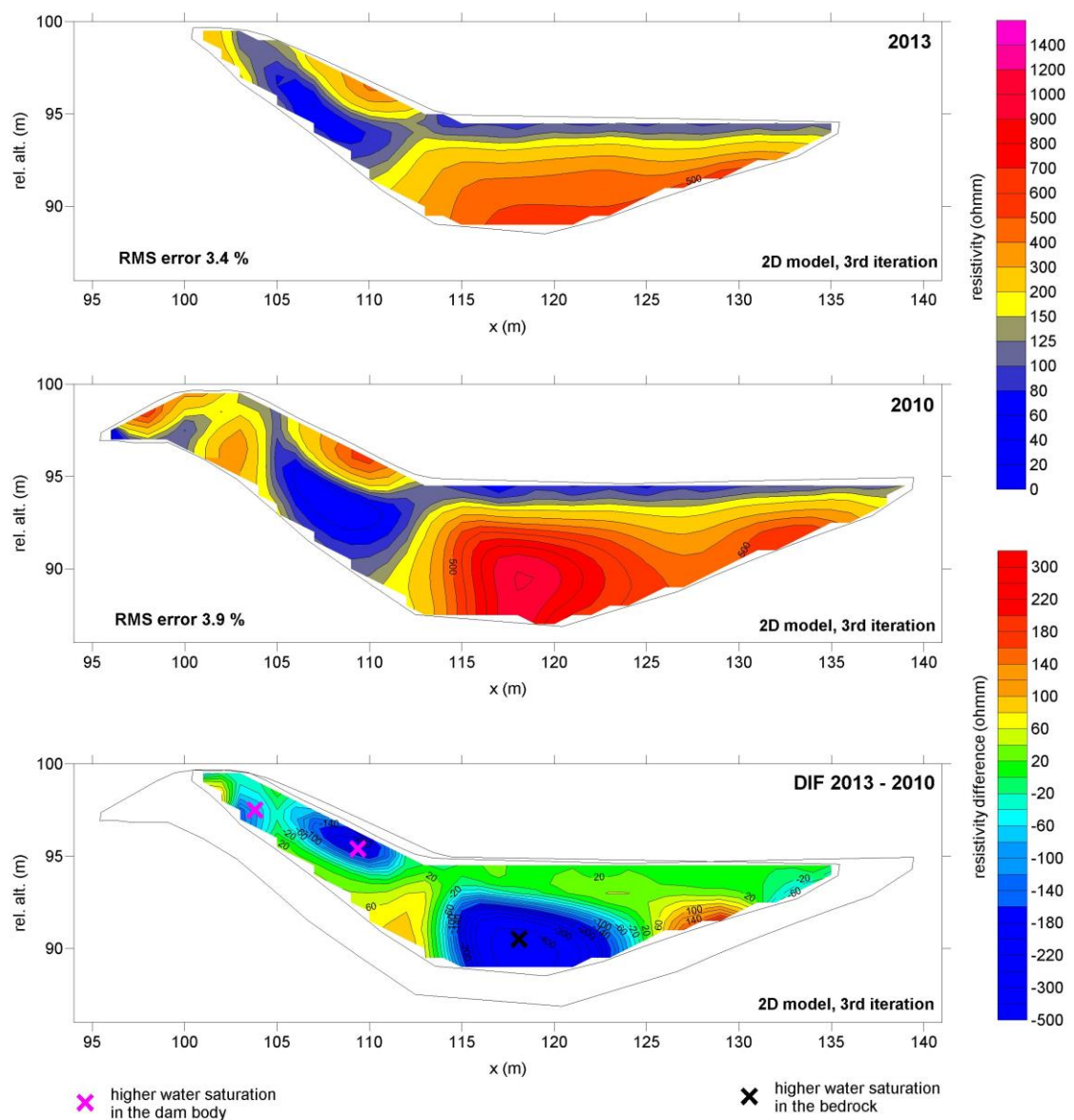
7 The seepage detection was checked with SP measurements too. Figure 13 shows  
 8 SP curves from the profile near the dam toe on the land side. There were zones with  
 9 significant changes of SP potential during the 2013 flood. In general, the data  
 10 obtained during flood were smoother due to high water saturation in the dam body.  
 11 All zones are in good correlation with the anomalies detected by the Slingram  
 12 method.



13  
14  
15  
16  
17

Figure 13. Graphs of SP potential for seepage detection. Profile at the dam toe on the land side.

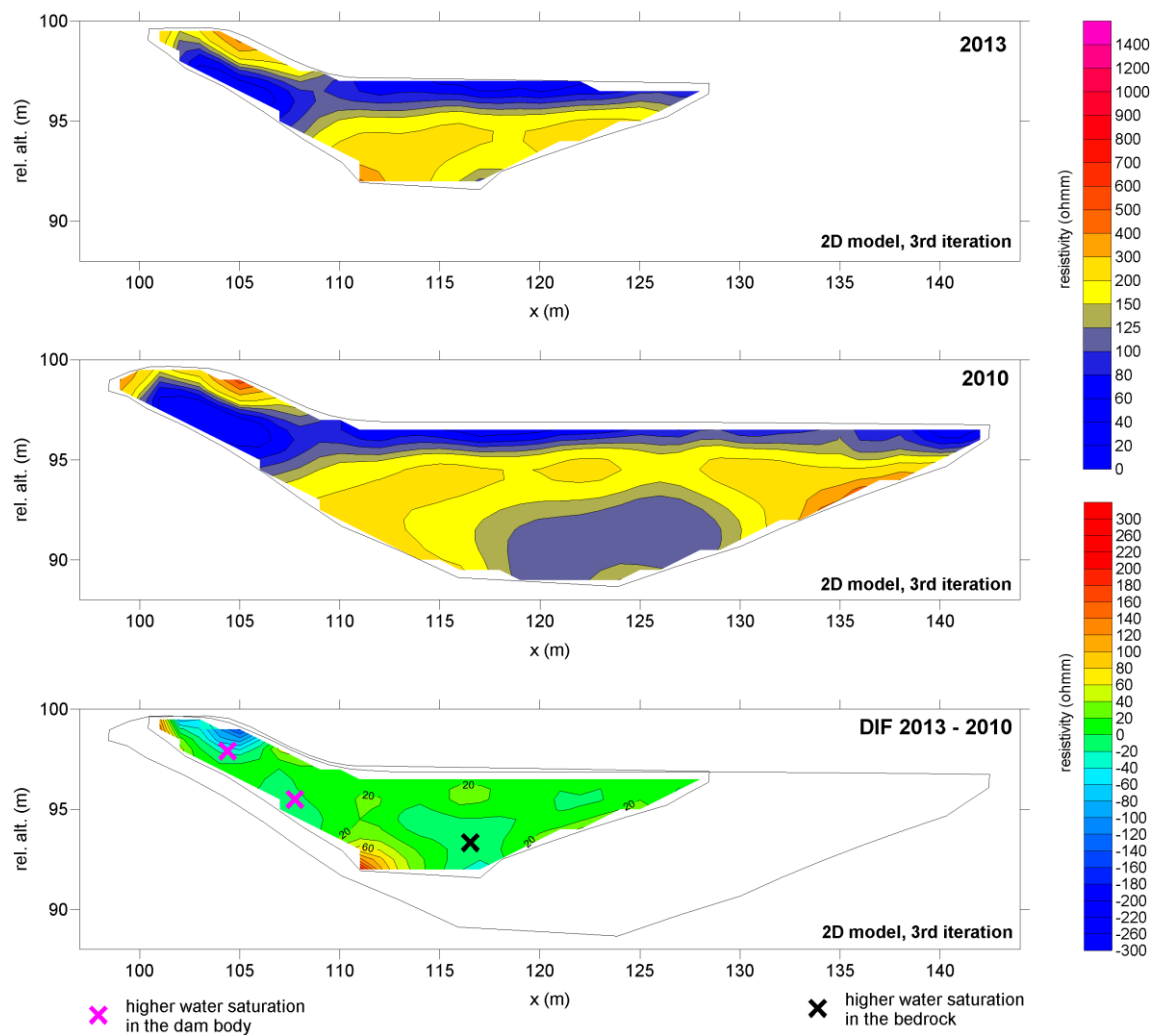
1 ERT measurements were carried out to refine the detection of changes in the dam  
 2 body in the zones previously discussed after the 2013 flood. The tomographic  
 3 subtraction showed on Figure 14a and Figure 14b revealed resistivity changes over  
 4 time between 2010 and 2013. In general, the ERT results showed good agreement  
 5 between the initial and repeated measurements. Near the main outlet, there was an  
 6 obvious decrease of resistivity in the dam body (Figure 14a), partly from the surface  
 7 due to saturation of soils after the rain, and in the bedrock zone under the dam. Both  
 8 anomalies were interpreted like a seepage effect around the outlet tube.



9  
 10  
 11  
 12  
 13

Figure 14a cross-section ERT. Perpendicular profile near the outlet, scans subtraction for the years 2010 and 2013.

1 The differential resistivity anomaly in the interpreted seepage zone (Figure 14b)  
 2 showed small changes. Nevertheless, the higher water saturation of the dam and  
 3 bedrock underneath the dam after flood 2013 is shown as lower resistivity contours.  
 4 The old outlet with the original wood tube was probably based at this location and  
 5 was used to supply water to small annex fish pounds near the main dam. The tube  
 6 was probably obstructed. Hence, It could have work as a seepage/piping preferential  
 7 pathway. A similar mechanism could have occurred with old roots from dead trees.



8  
 9  
 10 Figure 14b ERT cross-section . Perpendicular profile near interpreted seepage area.  
 11 Scans subtraction for the years 2010 and 2013.  
 12  
 13 The anomaly in the bedrock near the outlet (Figure 14b) is distinctively larger than  
 14 the seepage area. The cause may be due to the difference in sediment type in the  
 15 meadow and its bedrock. Sand and gravel predominate in the area of the outlet, the

1 bedrock is mainly made of orthogneiss. Loam and clay sand are mostly present in  
2 the seepage zone and weathered granite can be found in the bedrock. The resistivity  
3 changes between flood and dry season is higher in the area with sand and bedrock,  
4 as seen of Figure 14a.

5  
6

#### 7 **4. Conclusion**

8 By using all four techniques much more information is gathered than by individual  
9 techniques. The fact that these tests are all non-invasive means that the integrity of  
10 the embankment has not been breached. Furthermore these tests are far more  
11 economical than traditional trenching or borehole investigations and also the whole  
12 embankment is assessed and no hot spots are missed, which could have  
13 catastrophic results in both social and economic terms.

14 The value of using these combined techniques cannot be underestimated for both  
15 flood prevention and damage remediation. The quantity and quality of information  
16 covers fast scan assessment of the whole embankment which can identify weak  
17 zones or damaged zones not apparent by visual examination. These require further  
18 investigation which can be done by the application of high resolution techniques  
19 (ERT/SP/MG) at the specified locations.

20 The Slingram method is effective and fast and gave a basic description of material  
21 homogeneity and helped in the identification of the problematic zones. Self-Potential  
22 (SP) and Electrical Resistivity Tomography (ERT) provided the best interpretation of  
23 seepages with higher resolution. They were especially valuable when compared in a  
24 “time lapse” manner between the years 2010 and 2013. Changes in resistivity and  
25 conductivity related to drying or wetting process were subtracted after inversion. The  
26 zones affected by the resistivity changes could then be related to the post 2013 flood  
27 effect. On the other hand, the microgravimetry (MG) technique was able to detect  
28 the piping process with material transport and large cavity propagation and confirmed

1 SP and ERT results. The repeated measurements during changes in hydraulic  
2 regime (dry season versus flood events) made the interpretation of defects more  
3 accurate as proved on ERT time subtractions scans and Slingram, SP and MG  
4 comparative results between the year 2010 and 2013. Repeated geoelectrical  
5 measurement revealed the relative changes of water saturation in the selected  
6 reservoirs embankments. By using all four techniques together the assessor has a  
7 degree of certainty and confidence in the results meaning that the most appropriate  
8 and economical solution can be applied.

9

## 10 **Acknowledgments**

11 The authors wish to acknowledge the support of the European Commission via the  
12 Marie Curie IAPP project MAGIC - Monitoring systems to Assess Geotechnical  
13 Infrastructure subjected to Climatic hazards (FP7-PEOPLE-2012-IAPP-324426).

## 14 **References**

15

16 Beneš, V., Tesař M., Boukalová Z., 2011. Repeated geophysical measurement – the  
17 basic principle of the GMS methodology used to inspect the condition of flood control  
18 dikes. River Basin Management 2011 (25 - 27 May, Riverside, California, USA).

19

20 Castellanza, R., Utili, S., Galli, A., Sentenac P., 2014. An integrated  
21 geotechnical/geophysical approach for deterioration assessment of flood  
22 embankments. Journal of Geotechnical and Geo-environmental Engineering. 141 (3),  
23 04014111 pp 1-19

24

25 Chao, C. et al., 2006. Integrated Geophysical Techniques in Detecting Hidden  
26 Dangers in River Embankments. Journal of Environmental & Engineering  
27 Geophysics; v. 11; issue. p. 83-94; doi: 10.2113/JEEG11.2.83

1  
2  
3  
4  
5  
6  
7  
8  
9  
10  
11  
12  
13  
14  
15  
16  
17  
18  
19  
20  
21  
22  
23  
24  
25  
26  
27  
28

Cho, In-Ky., Yeom, Ji-Yeon., 2007. Cross line resistivity tomography for the delineation of anomalous seepage pathways in an embankment dam. *Geophysics* 72, G31; doi:10.1190/1.2435200

Cooling, L.F., Marsland A., 1954. Soil Mechanics Studies in the sea defence banks of Essex and Kent. Proceedings of the ICE Conference on the North Sea Floods of 31<sup>st</sup> January/1 February 1953.

Di Prinzioa, M., Bittelli, M., Castellarina, A., Rossi Pisab, P. 2010. Application of GPR to the monitoring of river embankments *Journal of Applied Geophysics*. Volume 71, Issues 2–3, Pages 53–61

Dyer, M.R., Utili, S., and Zielinski, M. 2009. Field study into fine desiccation fissuring at Thorngumbald. *ICE Proceedings. Water Management*, Issue WM3, pp.221-232

Griffiths, D.H., Barker, R.D., 1993. Two-dimensional resistivity imaging and modeling in areas of complex geology. *Journal of Applied Geophysics* 29, pp. 211–226.

Hadley, L. M., 1983. Geophysical Method of Evaluating Existing Earth Embankments *Bulletin of the Association of Engineering Geologists* Vol. 20, no. 3, pp. 289-295.

Jones, G., Sentenac P., Zielinski M., 2014. Fissure detection using 2-D and 3-D Electrical Resistivity Tomography on a flood embankment. *Journal of Applied Geophysics*. Vol.106, pp 196–211

Marsland, A., 1968. The Shrinkage and Fissuring of Clay in Flood Banks. Building Research Establishment, internal report No 39/68.

1

2 McDowell, P.W. et al., 2002. Geophysics in engineering investigations. Construction  
3 industry research and information association CIRIA C562. pp 252

4

5 Mydlikovski, R., Beziuk, G. and Szykiewicz, A., 2007. Detection of Inhomogeneities  
6 in Structure of Flood Embankments by Means of D.C. Resistivity, GPR and  
7 Frequency Electromagnetic Method Measurements . Acta Geodyn. Geomater., Vol.  
8 4, No. 4 (148), 83-88.

9

10 Nguyen, F., et al., 2005. Image processing of 2D resistivity data for imaging faults.  
11 Journal of Applied Geophysics, Volume 57, Issue 4, 260-277

12

13 Niederleithinger, E., Weller, A., and Lewis, R., 2012. "Evaluation of Geophysical  
14 Techniques for Dike Inspection." JEEG, 17(4), 185-195.

15

16 Reynolds, J.M. 1997. An Introduction to Applied and Environmental Geophysics. ,  
17 John Wiley and Sons, Chichester.

18

19 Sentenac, P., Jones, G., Zielinski, M., Tarantino, A., 2013. An approach for the  
20 Geophysical Assessment of Fissuring of Estuary and River Flood Embankments:  
21 Validation against two case studies in England and Scotland. Environmental Earth  
22 Sciences, Volume 69, Issue 6, pp 1939-1949.

23

24 Sjö Dahl, P., Dahlin, T., Zhou b., 2006. 2.5 D resistivity modeling of embankment  
25 dams to assess influence from geometry and material properties. Geophysics, V. 71,  
26 issue 3; G107-G114 doi:10.1190/1.2198217

27

1 Zielinski, M., Sentenac, P., McCloskey, G., Dyer, M. 2010. Desiccation cracking  
2 detection using resistivity array. ICE Proceedings. Geotechnical Engineering, GE-D-  
3 10-00068.

4

5

6

7

8

9

10

11

12

13

14

15

16

17

18

19

20

21

22

23

24

25

26

27